2018, 2023 CC-BY 4.0
https://doi.org/10.1002/essoar.10503117.1

Carbon Dioxide Removal Estimation Method to Remove Cumulative Anthropogenic CO_2 Emissions Distribution to Natural Sinks

Shannon A. Fiume
Open NanoCarbon, San Francisco, CA USA
Correspondence: shannon@autofracture.com

Abstract

We provide a method to estimate how to determine the amount of carbon to remove to affect the cumulative emitted anthropogenic carbon dioxide for Carbon Dioxide Removal (CDR) targets when climate modeling is unavailable. Additionally, comparing the growth in anthropogenic carbon dioxide emissions to the late-Holocene atmospheric carbon dioxide concentration for historical context and present hypothetical emissions declines for climate restoration. We explore the recent historical context of cumulative anthropogenic carbon dioxide emissions and how it has induced increases to each of the natural sinks: the oceans, atmosphere, and land. The magnitude of cumulative emissions is obscured when only considering yearly emissions change. A possible baseline CO_2 concentration of 280.9 ± 0.9 ppm for pre-human change stretching from 600 BCE to 1750 CE was found and could be explored separately. We show multiple speculative emission declines to zero cumulative CO_2 emissions to reach complete climate restoration. For groups seeking climate restoration, which completes in less than half a human lifespan, a pair of emission declines are presented, which complete in twenty years. The declines bound a possibility horizon of complete climate restoration ending with 2100 targets. There is a tradeoff between how fast the climate can be restored compared to how long humans can continue to emit carbon dioxide from the use of fossil fuels and land use change. We conclude with hypothesized climate reversibility through hypothesized emissions declines.

1. Introduction

As the Earth is a closed system, anthropogenic CO_2 emissions move to reside in natural sinks. Human activity from fossil fuel emissions and land-use change has radically increased the carbon composition of the Earth's natural sinks by exponential emissions increases since pre-industrial times.

The carbon dioxide between the atmosphere and oceans sinks are balanced by atmospheric chemistry: atmospheric CO_2 exerts pressure on CO_2 dissolved in the ocean surface waters (Takahashi et al., 2002). When CO_2 is removed from the atmosphere, the reduced CO_2 pressure allows the dissolved CO_2 remaining in the surface waters to outgas back to the atmosphere. Even though only about 50% of anthropogenic carbon stored in the ocean sink is in the top 400 meters (Sabine et al., 2004), the top 100 meters of surface waters contain the highly bioactive euphotic zone and is strongly negatively impacted by induced warming and acidification from anthropogenic carbon, additionally causing extensive damage to the marine ecology. Carbon dioxide dissolved in surface waters should be moved to more permanent storage to stop affecting the surface waters or atmosphere.

The exponential forcing of cumulative emissions is an important factor to emphasize, as it is not readily apparent in reporting yearly emissions change. Even considering an uncertainty of ±5% at a medium confidence level of the estimated cumulative anthropogenic emissions of 432 gigatonnes carbon (GtC) through 2017 per the Global Carbon Budget 2017 (Le Quéré et al., 2018), there is a significant difference between achieving SSP 1 1.9 (IMAGE), which could lower cumulative emissions to about 663 GtC and 0 GtC. Additionally, complicating removal efforts is how to determine the entire amount of carbon

2018, 2023 CC-BY 4.0
https://doi.org/10.1002/essoar.10503117.1

dioxide to remove. Without considering the carbon dioxide from all sinks and the rebalancing that occurs when carbon dioxide is removed from a sink, only converting atmospheric carbon dioxide concentration in ppm for a removal target leads to drawing down only the atmospheric sink.

When climate modeling is unavailable, in order to more accurately estimate the amount of carbon dioxide to remove for Carbon Dioxide Removal (CDR) and, ultimately, climate restoration, we examine the total accumulation of carbon to the natural sinks from anthropogenic carbon dioxide emissions. We compare the differences between cumulative and yearly changes in emissions and complete cumulative anthropogenic removal and highlight possible misinterpretation in solely examining yearly changes in emissions. We then provide estimates on highly speculative carbon removal emission declines. This work does not prescribe how carbon dioxide can or should be removed from the atmosphere. Determining the appropriateness of a given CDR technology over another or constructing a blend of technologies is beyond the scope of this work. This work exclusively focuses on greenhouse gas carbon dioxide calculations for climate restoration and CDR and does not cover other greenhouse gasses.

2. Anthropogenic Emitted Carbon, What and Where?

Over the years, fossil fuel emissions from humans burning carbon-based fuels have shifted between three major natural carbon sinks: land, ocean, and the atmosphere. Including the latest 2017 estimates, the total emitted carbon from anthropogenic CO_2 since 1750 is 627 GtC, where 432 GtC is from fossil fuel emissions and 195 GtC from land-use change (Le Quéré et al., 2018). The atmosphere currently holds about 271 GtC (Dlugokencky et al., 2018) in anthropogenic emissions. Emissions from anthropogenic land use change roughly equal the anthropogenic portion of the land sink. The natural sinks contain more carbon than the introduced anthropogenic carbon. This work only focuses on the increases to the total carbon in the natural sinks from anthropogenic emissions sources. Carbon quantities are listed in gigatonnes carbon (GtC) or the equivalent petagrams carbon (PgC). To obtain gigatonnes CO_2, multiply by a conversion factor of 3.664 (Le Quéré et al., 2018).

Total Cumulative Anthropogenic Emissions	Fossil Fuel Emissions	Land-use Change Emissions	Land Sink	Ocean Sink	Atmospheric Sink*	Budget Imbalance
627.1	431.6	195.5	-189.8	-157.5	-271.3	-8.5

Table 1 | All values are from the Global Carbon Budget (Le Quéré et al., 2018) except the Atmospheric Sink. The atmospheric sink was generated from the current Global CO_2 Concentration from Mauna Loa (Dlugokencky et al., 2018) and converted to GtC via subtracting 277 ppm and multiplied by the conversion factor 2.12 (Ballantyne et al., 2012).

The year-to-year change in cumulative anthropogenic fossil fuel emissions results in strong exponential growth that is highly correlated to carbon growth in atmospheric, ocean, and land sinks. Figure 1 plots the cumulative anthropogenic carbon from fossil fuels and land-use change CO_2 emissions per year and how that carbon dioxide is distributed to the natural sinks. To complete the atmospheric dataset, the Keeling Curve is shown in light blue, overlaying the cumulative atmospheric yearly growth from the Global Carbon Budget 2017 (Le Quéré et al., 2018). The Keeling Curve is the globally averaged CO_2 concentration measured at Mauna Loa from 1980 to 2017 (Dlugokencky et al., 2018) and was converted to GtC by the conversion factor 2.12 (Ballantyne et al., 2012). Natural sink curves also show slower-growing exponential curves. The steepest part of the cumulative fossil fuel emissions curve happened within the last two decades.

2018, 2023 CC-BY 4.0
https://doi.org/10.1002/essoar.10503117.1

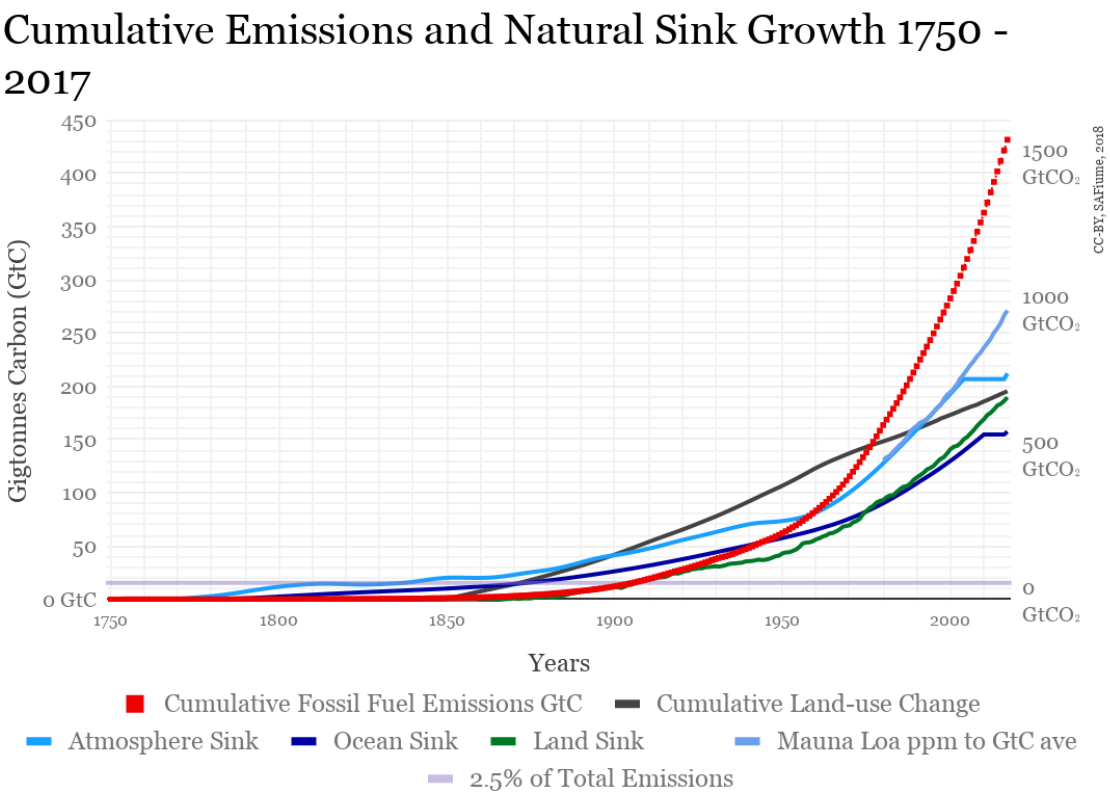

Figure 1 | After 1750, anthropogenic emissions experienced exponential growth, and starting around the 1850s, human-induced land-use change experienced close to linear growth. The natural sinks have experienced related exponential growth. Data points are from the Global Carbon Budget (Le Quéré et al., 2018) except where noted. Not all data points have values prior to the 1860s. The ocean and atmospheric sinks have additional gaps starting in 2005 onward. The break for the atmospheric curve is completed by the overlay of the globally averaged Mauna Loa Keeling curve displaying anthropogenic emissions (value parts per million volume - 277 ppm) for the time period 1980-2017 and converted to GtC with the stock conversion factor of 2.12.

The Global Carbon Budget 2017's Equation:

$$E_{ff} + E_{luc} = G_{atm} + S_{ocean} + S_{land} + B_{bim} \quad , \qquad [1]$$

(Le Quéré et al., 2018) states the yearly growth of fossil fuel and land-use change emissions are equal to the total yearly growth in CO_2 concentration for all natural sinks: atmosphere, ocean, and land sinks. This yearly growth rate, equalling the aggregate of all the natural sink's yearly growth rate, can be expanded to the total cumulative emissions, equalling the cumulative anthropogenic carbon distributed to the combined natural sinks. Where the GCB equation concerns yearly flux, Equations 2, 3, show the cumulative emission sources are equal to the total accumulated anthropogenic carbon since 1750 distributed among the three sinks though a given year n:

$$E_{\Sigma ff_n} = \sum_{i=1750}^{n} E_{ff_i} \quad , \qquad [2]$$

$$E_{\Sigma ff_n} + E_{\Sigma luc_n} = A_{atm\ sink_n} + A_{ocean\ sink_n} + A_{land\ sink_n} \quad . \qquad [3]$$

From the Equations 1-3, we can see the total anthropogenic atmospheric CO_2 concentration (through a given year n) is the total atmospheric CO_2 concentration minus the year 1750's CO_2 concentration of 277 ppm. Multiplying the current anthropogenic CO_2 ppm by 2.12 (Ballantyne et al., 2012) yields the anthropogenic carbon content in GtC.

The relationship between the total carbon emitted and how it is distributed to each natural sink is shown in Figure 2, by stacked columns of cumulative anthropogenic fossil fuel and land-use change emission sources and Earth's three natural

sinks. The negative quantity of the natural sinks shows the amount of carbon that ought to be removed to balance out the total amount of carbon emitted. The oceanic anthropogenic carbon is roughly 58% of the atmospheric anthropogenic carbon or approximately 36% of the total emitted from fossil fuel emissions. The atmospheric anthropogenic carbon accounts for the remaining 63% of fossil fuel emissions.

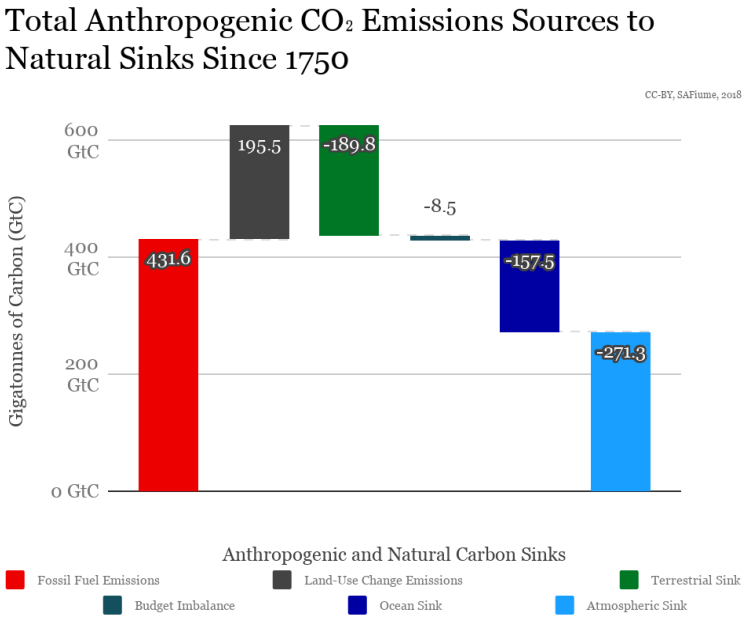

Figure 2 | Emissions sources are distributed nearly 36% to the ocean and 63% to the atmosphere, assuming Land-use change roughly equals the land sink. The budget imbalance is due to carbon missing from a natural sink, possibly from seasonal change and differing accounting methods.

Total anthropogenic carbon emissions experienced strongly accelerating growth compared to the stable historic CO_2 concentration. Figure 3 is a composite graph of CO_2 concentration data from multiple Antarctic ice core studies performed on Dome Concordia (Dome C) (Luethi et al., 2008; Flückiger et al., 2002; Monnin et al., 2001), Vostok Dome (Siegenthaler et al., 2005; Pépin et al., 2001; Petit et al., 1999;), Taylor Dome (Indermühle et al., 2000), WAIS Divide (Bauska et al., 2015), Maud Dome and the South Pole (Siegenthaler et al., 2017), and Law Dome (Etheridge et al., 1996; MacFarling Meure et al., 2006 and MacFarling Meure 2004), stretching for about two thousand years, from 600 BCE to 2004 CE and completed with the globally averaged CO_2 concentration from Mauna Loa from 1980 CE - 2017 CE, resulting in the top adjoined blue curves. The atmospheric curve has been shifted upwards to start above the top of the ocean sink curve. The mean CO_2 concentration of 280.9 ± 0.9 ppm for 600 BCE to 1750 CE is shown in light green. The left axis has been calibrated to set 281 ppm equal to 348 GtC such that the green line meets 190 GtC - the top of the land curve added to 158 GtC - the top of the ocean curve. The curve in red is the total anthropogenic emissions from both fossil fuel and land-use change. The dark blue and green lines are the ocean and land sinks, respectively, which are cumulatively stacked below the atmospheric curve to illustrate the relationship to total carbon emissions. The top blue line does not meet the red emissions curve due to the budget imbalance.

2018, 2023 CC-BY 4.0
https://doi.org/10.1002/essoar.10503117.1

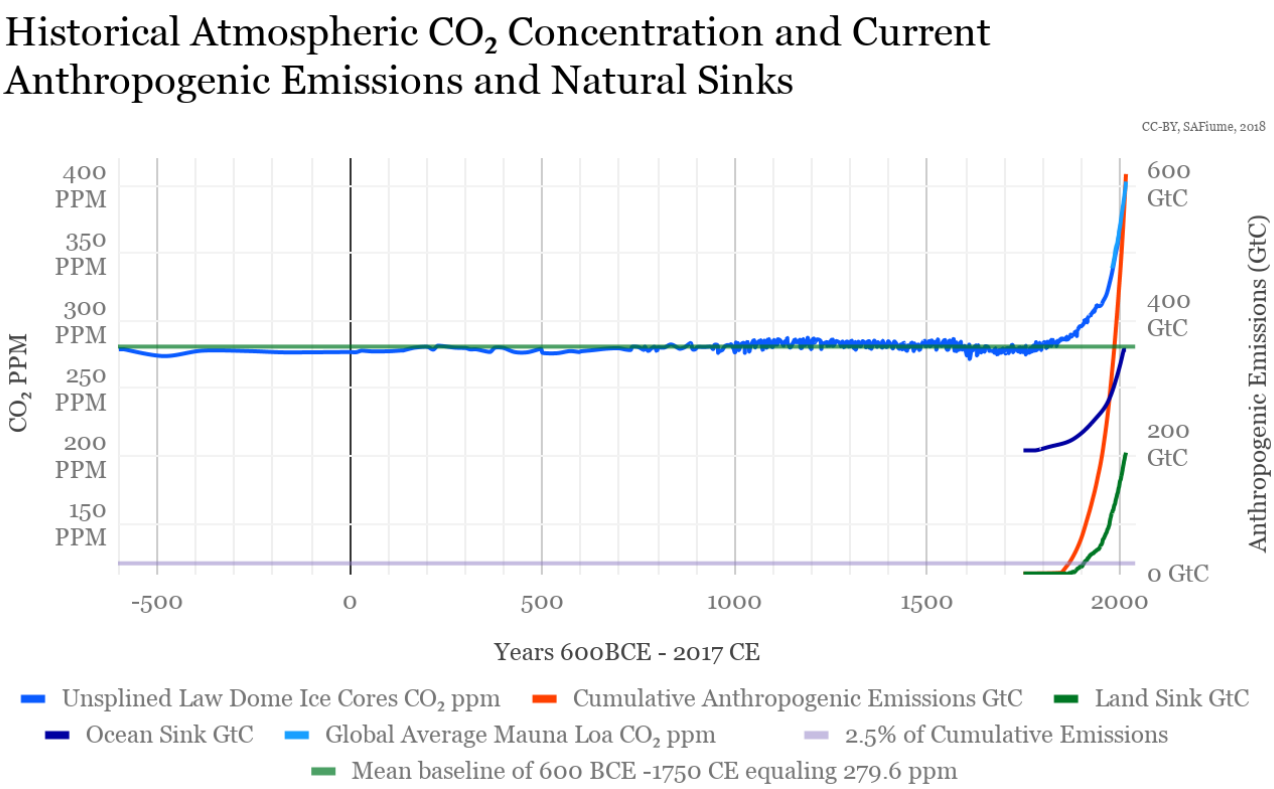

Figure 3 | Historical atmospheric CO_2 concentration is shown stacked above the ocean and land sink totals. The ice core CO_2 concentration data is from Dome C (Monnin et al., 2001; Luthi et al., 2008), raw Law Dome data points (Etheridge et al., 1996; MacFarling Meure 2004; MacFarling Meure et al., 2006), WAIS Divide (Bauska et al., 2015), Maud Dome and the South Pole (Siegenthaler et al., 2017). Law Dome data from the present reads slightly lower ppm than Mauna Loa's global average. The data to generate the graphs are open and listed in the Data Availability section. Cumulative anthropogenic emissions from fossil fuels and land-use change total 627 GtC and start picking up in the mid-1800s. The line in light purple is 2.5% of total emissions, about 15.7 GtC. The light green line is the mean CO_2 concentration equaling 281 ppm from 600 BCE to 1750 CE. The axes are calibrated such that 113.18 ppm equates to 0 GtC of anthropogenic emissions increases.

The line in light purple corresponds to 2.5% of 627 GtC, or total anthropogenic emissions for both land-use and fossil fuel emission, equalling about 15.7 GtC, or 284 ppm.

The baseline of 277 ppm is the mean ppm for the time 1739 to 1772 CE. To check that this concentration was not a local minimum for only that time span, the historical CO_2 concentration was examined and shown in Figure 4. Antarctic ice cores from Law Dome, Dome C, Maud Dome, Taylor Dome, WAIS Divide, Vostok, and the South Pole yielded that CO_2 concentration has varied only slightly, ranging from 182.2 ppm to 287.5 ppm, for 137,000 BCE to 1750 CE. For modern times, CO_2 concentration has been stable since 1750 to about 600 BCE. Before 600 BCE, the concentration slowly trends lower than 275 ppm, eventually dropping to 184 ppm. A mean from the ice core samples gives a baseline of 280.9 ± 0.9 ppm for the recent stable past of 600 BCE to 1750 CE.

2018, 2023 CC-BY 4.0
https://doi.org/10.1002/essoar.10503117.1

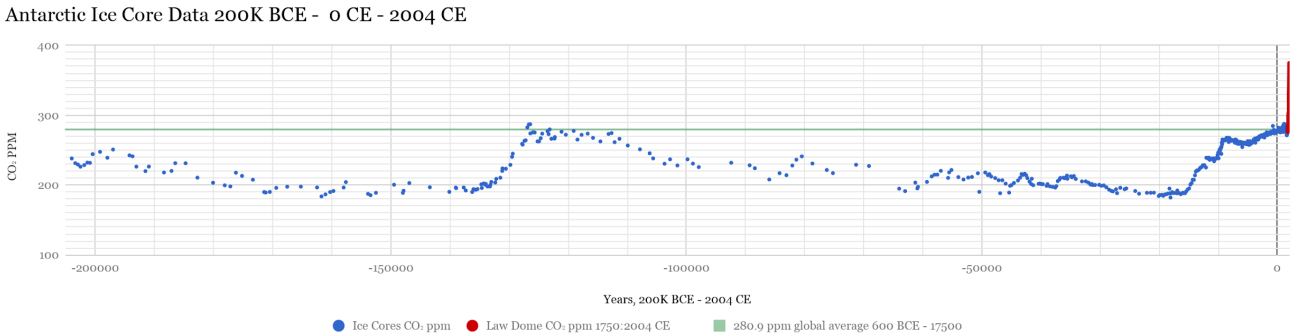

Figure 4 | Scatter plot of Antarctic Ice Core CO_2 concentration data from multiple ice cores: Law Dome, Dome C, Maud, Taylor Dome, WAIS Divide, Vostok, and the South Pole from the time of 125000 BCE to 2004 CE. The pale green line is the mean of 280.9 from 600 BCE to 1750 CE.

Given the exponential forcing from the total cumulative emissions, the line in purple from Figure 3 represents a potential safe region to reduce major CO_2 concentration increase from outgassing. However, it is also possible the only safe region to prevent major CO_2 concentration increases from outgassing is the total removal of all cumulative anthropogenic emissions since 1750.

3. Estimating the Carbon Dioxide to be Removed

By removing carbon dioxide from the atmosphere, we can change the atmospheric CO_2 concentration. If only the anthropogenic emissions were removed from the atmospheric sink, as shown in Figure 2, equalling 271.3 GtC, the hundreds of gigatonnes of carbon remaining in the ocean and land sinks would outgas and diffuse to transfer some of the anthropogenic-sourced CO_2 back to the atmosphere. Specifically, if we were to remove 271.3 GtC,

$$627.1\,GtC - 271.3\,GtC = 355.8\,GtC \quad , \qquad [4]$$

or

$$431.6\,GtC - 271.3\,GtC = 160.3\,GtC \quad , \qquad [5]$$

we would still have a remaining 356 GtC in the ocean and land sinks shown in Equation 4, or 160 GtC, assuming the land-use change is roughly equal to the land sink shown in Equation 5, and also illustrated in Figure 2. Still assuming the land-use change is roughly the same as the land sink, the natural rebalancing would move atmospheric CO_2 concentration from 277 ppm upwards, depending on how much the land sink outgasses. We last reached 160 GtC during 1980, when cumulative fossil fuel emissions ended the year at 164 GtC. After we reach a desired atmospheric concentration level, we need to continue to remove additional carbon dioxide to lower the anthropogenic carbon diffused in the ocean surface waters.

2018, 2023 CC-BY 4.0
https://doi.org/10.1002/essoar.10503117.1

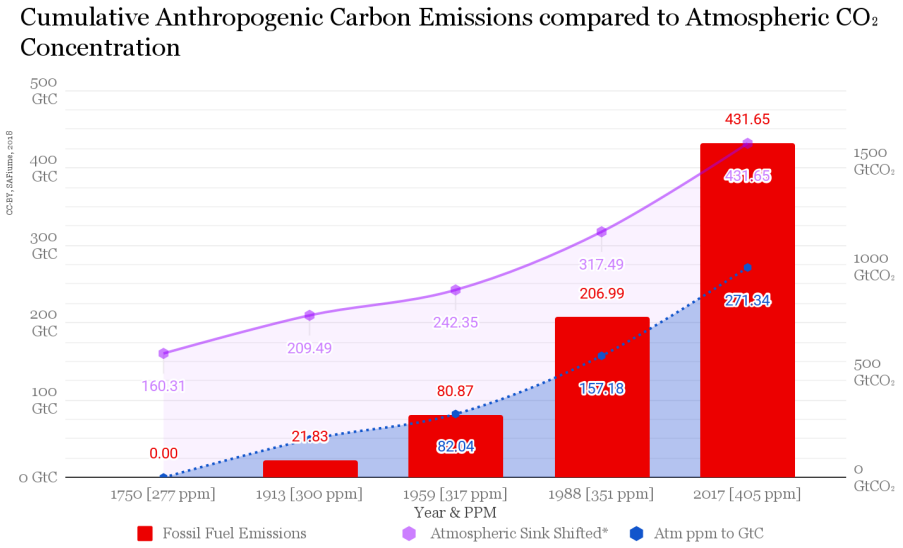

Figure 5 | Fossil Fuel Emissions (GtC) and CO_2 ppm concentration converted to GtC for the years 1750, 1913, 1959, 1988, and 2017. The horizontal axis scaling is not to scale and hides the exponential extent of these curves. For ease of illustration, the global average Atmosphere CO_2 ppm converted to GtC then shifted to drop from the top of fossil fuel emissions for 2017, see Equation 5. When removing carbon only by the direct conversion of ppm to GtC leads to significantly undercounting the remaining anthropogenic carbon.

To illustrate the undercounting by the plain conversion of ppm to GtC of an atmosphere portion, we'll examine a common target of 350 ppm. 350 ppm was roughly seen in 1988 when atmospheric emissions were 157.18 GtC, and subtracting from 2017's concentration equals 114.16 GtC.

$$(404.99\,ppm - 351.14\,ppm) * 2.12\,GtC/ppm = 114.16\,GtC \quad , \qquad [6]$$

$$431.65\,GtC - 114.16\,GtC = 317.49\,GtC \quad . \qquad [7]$$

The data point in Figure 5 for 1988 [351 ppm] is 317.49 GtC or 114.2 GtC lower than 431.6 GtC. If we remove 114.2 GtC shown in Equation 6, we will not lower anthropogenic emissions to the anthropogenic attribution for 1988 (206.99 GtC), and the remaining anthropogenic carbon would likely increase upwards above 350 ppm from the ocean and possibly land outgassing.

For a rough estimate of anthropogenic carbon quantities when sufficient modeling is unavailable, we refer to the historical anthropogenic emissions to include the anthropogenic carbon distributed to each natural sink. To illustrate how to determine how much carbon to remove, find the year the desired ppm or emissions occurred, then take the current cumulative emissions and subtract the historical cumulative emissions for that year. For 350 ppm, the actual removal should be as shown in Equation 8:

$$431.6\,GtC - 207.0\,GtC = 224.6\,GtC \quad . \qquad [8]$$

Note that 350 ppm is significantly far from the baseline of 280.9 ppm and represents about 207 gigatonnes of carbon that was not previously in the atmosphere or oceans since the mid-Pliocene warm period or about 3.2 MyBP (million years before present, or million years since 1950 CE) (Raymo et al., 1992).

Figure 6 shows the cumulative stacking of all the natural sinks and emissions sources for five individual years. The atmospheric sink in the dashed purple line drops from the fossil fuel emissions, ending at 160.3 GtC and closely matching the ocean sink at 157.5 GtC. The exponential increase in emissions radically increases the amount of carbon that ought to be removed to stabilize Earth's climate.

https://doi.org/10.1002/essoar.10503117.1

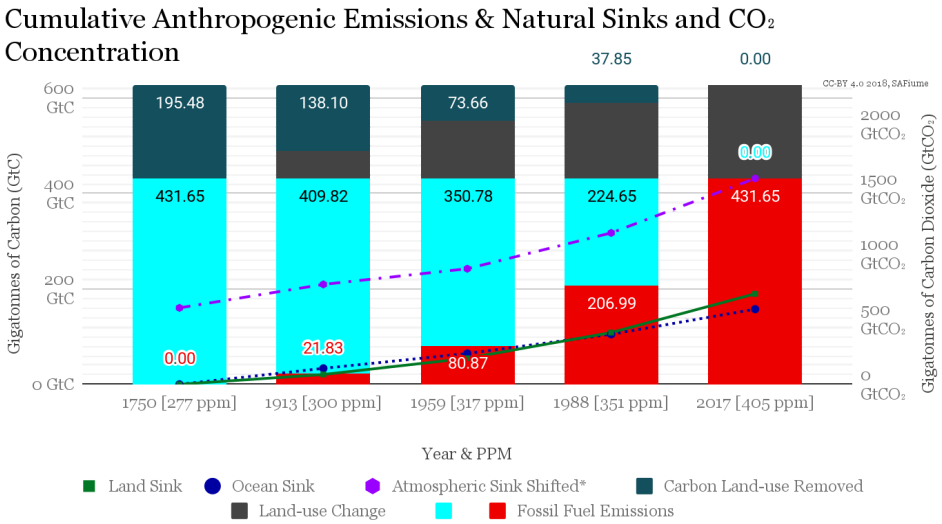

Figure 6 | This graph shows a conversion of ppm to GtC shifted to descend from 431.6 GtC, and the rate increase for the natural sinks over time. It has stacked columns of fossil fuel, land-use change emissions, and carbon removal targets for the years: 1750, 1913, 1959, 1988, and 2017, corresponding to 277, 300, 317, 351, and 405 ppm, and natural sink growth. CO_2 ppm concentration is converted to GtC. The Carbon Removal is the total amount of carbon that would have to be removed to restore the carbon dioxide concentration in all sinks and emissions for that time. If we remove a total of 409.8 GtC and also 174 GtC from land-use change emissions, we would achieve 300 ppm, last seen in 1913.

"We infer from Cenozoic data that CO_2 was the dominant Cenozoic forcing, that CO_2 was ~450 ± 100 ppm when Antarctica glaciated, and that glaciation is reversible." (Hansen et al., 2008) The error margin of 100 ppm is wide enough to place reverse glaciation possible at 350 ppm. Given the radical nature of the exponential increase from 277 ppm and temperature increase from pre-industrial times, 350 ppm is not likely to yield a long-term stable climate.

Given the magnitude of outgassing by the three sinks, effort should focus on removal of the total cumulative anthropogenic carbon for a given time period to achieve a specific CO_2 concentration. To achieve 277 ppm, focus on removing total cumulative anthropogenic emissions (approximately 1.5 trillion tonnes of CO_2, Eq. 5), and possibly forcing the land sink to zero emissions (approximately totalling to 2.4 trillion tonnes of CO_2, Eq. 4), not by only removing 272 GtC (approximately 1 trillion tonnes of CO_2).

3.1 Comparison with Yearly Change

To better visualize the magnitude of growth in total emissions, total cumulative carbon emissions were graphed as opposed to the year-to-year change in emissions. Figure 7 shows the yearly change in emissions more commonly seen in papers comparing the Shared Socioeconomic Pathways (SSPs)(Riahi, et al., 2016). The yearly change graph hides the exponential nature of emissions curves and does not easily show how much carbon may need to be removed to restore climate to a desired emissions target. For illustration in Figure 7, the SSP1 IMAGE RCP 2.6 by the IMAGE group (van Vuuren, 2016) was modeled and shown in yellow with the existing sinks and emissions data as well as four possible hypothesis emission declines to zero cumulative emissions. The SSP1 IMAGE RCP 2.6 is the marker scenario for SSP1: under this scenario, CO_2, along with all other GHG emissions, peak gradually and then drop (SSP Public Database version 1.1, 2018, van Vuuren, 2016). The SSP1 IMAGE RCP 2.6 emissions data spline was extrapolated from the emissions per decade, starting from 2010 to 2100, and including emissions from 2005 as listed from the SSP database.

In Figure 7, it is not readily apparent what cumulative emissions will be at the end of SSP 1 2.6 and emission declines. Our hypotheses emissions declines drop down to zero cumulative emissions in 2040 and 2100 (shown in detail in Figure 8), whereas the IMAGE SSP1 RCP 2.6 drops cumulative fossil fuel emissions down to about 870 GtC, roughly equivalent to total radiative forcing 2.6 W/m^2 and holding carbon dioxide concentration to about 430 ppm by the end of 2100.

2018, 2023 CC-BY 4.0
https://doi.org/10.1002/essoar.10503117.1

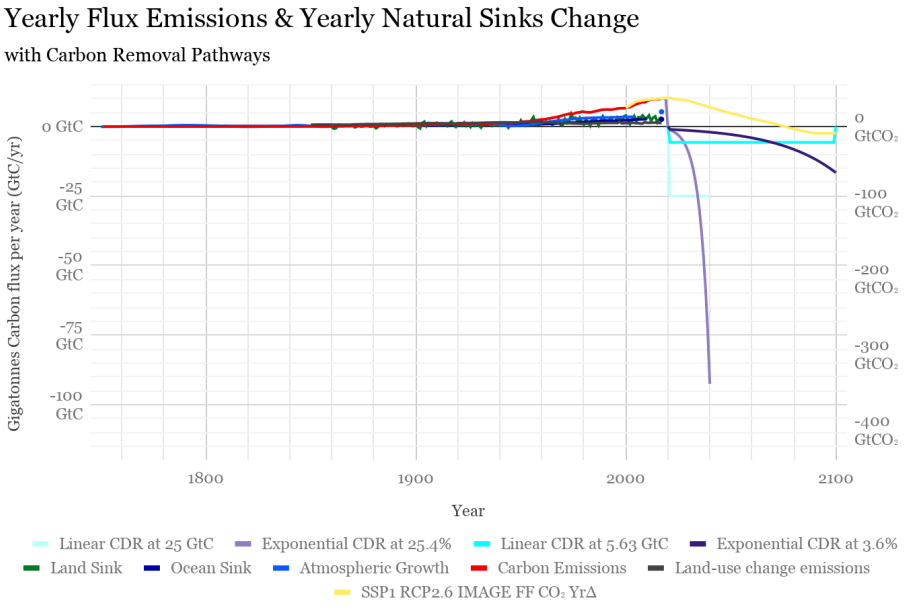

Figure 7 | This is the yearly graph of emissions and sink change. Included are the emission declines for carbon removal to achieve zero cumulative emissions. Most of the standard SSPs cross zero GtC after 2040 and end by 2100 or later. The SSP1 RCP26 IMAGE shows Fossil Fuel CO_2 emissions from the SSP database. The SSPs reach the warming target of 2ºC to 1.5ºC above Earth's temperature since the 1860s. The SSPs only remove some portion of carbon to equal the given radiative forcing and not all anthropogenic emissions. Although SSP1 IMAGE RCP 2.6 drops below zero yearly emissions, it does not reach zero cumulative emissions.

SSP1 IMAGE was modeled using MAGICC 6.0 (Meinshausen, M. 2011), which internally starts cumulative emissions from 1765 CE. Figure 8 lists SSP1 IMAGE RCP 2.6 yearly cumulative fossil fuel emissions change modeled on cumulative fossil fuel starting from levels in 2000. It also uses the extrapolated emissions data spline for SSP1 IMAGE RCP 2.6, like in Figure 7. All the emission declines and the SSP are carbon dioxide fossil fuel emissions, not the combined GHGs: $CO_{2\text{-eq}}$.

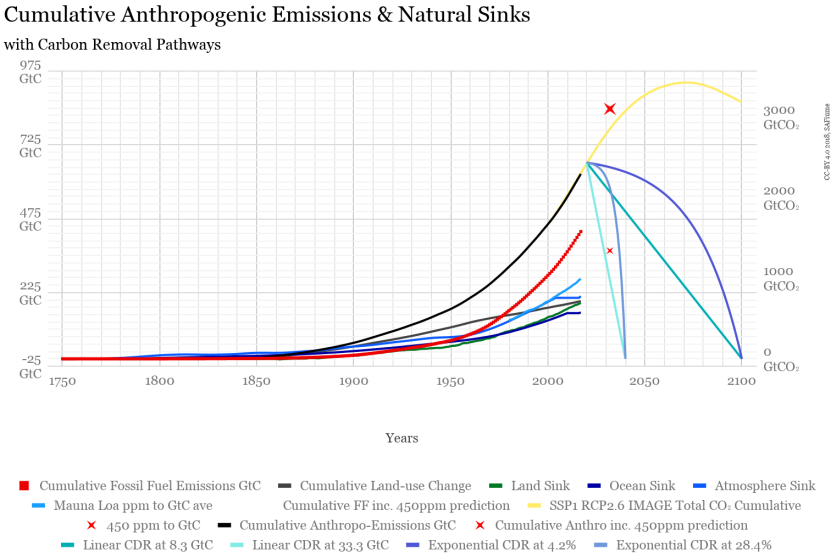

Figure 8 | Also included is the marker scenario for SSP 1: IMAGE RCP 2.6, shown in the yellow line. IMAGE RCP 2.6 scenario ends with a radiative forcing of 2.624 and 430 ppm CO_2-eq (SSP Public Database version 1.1, 2018).

2018, 2023 CC-BY 4.0
https://doi.org/10.1002/essoar.10503117.1

Given the exponential forcing of emissions, some small region starting at 277 ppm, possibly up to 300 ppm, is likely to lead to a stable climate with little to no outgassing from the other sinks. 300 ppm (last seen in 1913 when fossil fuel emissions were 22 GtC, and land-use change was 57 GtC) and less should be investigated to find the determining factor or Earth system configuration for climate stability. The investigation model or hypothetical should be able to set carbon concentration simultaneously within all sinks: atmosphere, ocean, and land, and also model large volume carbon removal over periods of ultrashort, short, medium, and long time frames.

Since the direct consequence of lowering CO_2 concentration results in outgassing and as the fossil fuel emission curve is a steep exponential of growing carbon, climate stability likely depends on achieving a slight to zero percentage of fossil fuel emissions. By removing the total amount of carbon, it should additionally force the ocean sink to become more alkaline compared to the present. Removing all accumulated anthropogenic carbon should return the natural albedo cooling and natural restoration of the cryosphere; the caveat is that the decline's cumulative and peak emissions must never exceed a value that would exceed the climate tipping points.

As the originating source emissions and subsequent natural sinks are exponentially increasing, at our current growth rate of 2% per year, we will likely reach 450 ppm during 2032, as shown in Figure 8. This extrapolation is based on continued fossil fuel emissions at a 2% yearly growth rate and extrapolating the time it takes for the atmosphere to reach 450 ppm, shown in the little red X, and also to the black cumulative fossil fuel plus land-use change curve shown in the large red X. As the extrapolation only considers anthropogenic emissions increases and does not take into account possible sudden warming from the loss of the Greenland Ice sheet and unlocking of frozen methane in the permafrost, a more realistic projection is likely much sooner than 2032. We have little time to hit peak yearly emissions and then to hit zero yearly emissions.

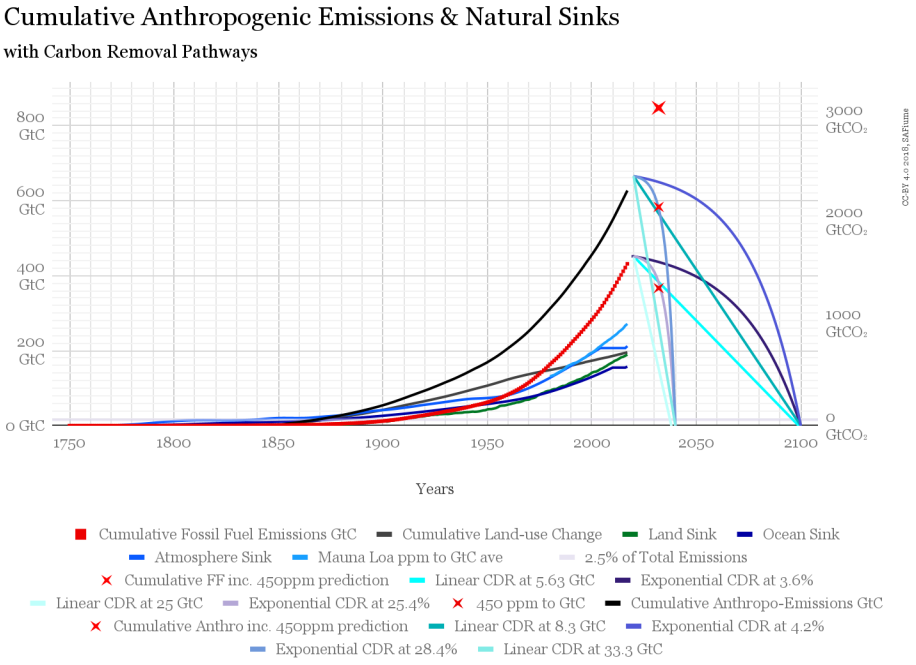

Figure 9 | Cumulative Anthropogenic Emissions & Natural Sinks and Emission declines to zero cumulative emissions. 450 ppm is extrapolated from the Mauna Loa curve and shown in the red X. Translating that extrapolation to the fossil fuel and fossil fuel plus land-use curves assuming a continued yearly growth rate of 2% gives the red Xes. The red Xes are projected to occur in 2032. The emissions declines bound CDR in a minimum and maximum effort range to target what is possible and do not account for a price on carbon or price to deploy a given technology, which is embedded in some Pathway models. Efforts between the teal and purple lines would keep the climate radically below 1.5ºC. Efforts between the teal and purple lines that end at something less than 20 GtC would reset climate levels prior to the climate of the early 1900s. Efforts that reach zero and are between the teal and purple lines would reset the climate back to levels last seen in 1750.

2018, 2023 CC-BY 4.0 https://doi.org/10.1002/essoar.10503117.1

4. Possible Emission Declines to Zero Degrees Warming

Four hypothetical emission declines are presented to show linear and exponential declines to bound removal in a minimum and maximum timeframe. In Figure 9, a zero-degree warming emission decline can be achieved by the curves in shades of cyan or purple. A possible maximum cumulative emissions removal is shown spanning eighty years. The cyan line is a hypothetical linear carbon removal of 5.8 GtC per year for eighty years, starting at 500 GtC. By 2080, there would only be about 115 GtC left to remove. Depending on how the CO_2 concentration was split between the sinks, the oceans should see significant recovery and slight global cooling by 2080. The dark purple curve shows an exponential decline of 3.5%, starting from 461 GtC in 2020 and finally trending to below zero in 2100.

For climate restoration in less than half a human lifespan, the pale lines show hyper-aggressive carbon removal in twenty years. The pale purple shows an exponential decline of 27.5%, starting from 451 GtC in 2020 and finally trending to below zero in 2040. The pale cyan shows a linear removal of 25 GtC per year for twenty years, and 125 GtC would be remaining at year fifteen. How fast the oceans recover or permafrost regenerates in response to an abrupt drop in CO_2 concentration should be explored. In an abrupt CO_2 concentration drop scenario, solid carbon could additionally be distributed to the land sink to keep the land sink absorption high.

These emission declines are a simple removal of carbon and do not consider a price for carbon or the price to implement a given carbon removal method, which is in some of the advanced modeling tools for analyzing Pathways. These simpler estimated declines outline a rough guideline of what we can remove and provide a rough check for the model output, additionally, a more advanced climate model ensemble of calibrated models and experiment parameters can better forecast the future given Earth's present climate.

The exponential declines mimics a slow exponential increase in reduction in carbon emissions. Exponential curves are more similar to a rapid technology adoption model or crash in price from technological improvements and follow Moore's Law.

5. Data Availability

All data and graphs are available in the open google spreadsheet: Total Emitted Carbon Graphs and Comparisons. The tabs contain SCEN data that can be converted to CSV files to be imported to MAGICC. The hypothetical declines were imported to MAGICC 6.4 and live.magic.org to allow a finer detailed comparison. The MAGICC 6.x SCEN files for declines are available at the google drive location. SSP1 IMAGE RCP 2.6 data was obtained at the SSP Public Database version 1.1 and generated in 2018. This paper is open and licensed under the Creative Commons CC-BY 4.0 International License.

6. Conclusion

Creating CDR targets from cumulative emissions totals should quicken climate restoration of the polar regions as they focus on removal of emissions rather than holding to a given warming level. Emissions diffused in surface waters and their complex interaction with ocean mixing and the atmospheric sink justifies a more involved approach to generating CDR targets rather than a plain conversion of atmospheric ppm to bulk carbon. Although obscured when only considering a radiative forcing level or purely looking at the yearly change in emissions, the exponential nature of cumulative growth in emissions shows significant growth throughout the 1980s to the present and mirrors much of the deployment growth of information advances. Given the exponential nature and magnitudes larger than zero cumulative emissions, the effects of CDR to 22 GtC fossil fuel added to 57 GtC land-use change ranging to CDR to zero cumulative emissions with shorter than 80-year timeframes or ending in the year 2100 would highly benefit from additional study. Given the vast amounts of carbon that need to be removed for complete climate restoration, carbon dioxide removal technologies, geo-engineering, bio-engineering, and other engineering and processes comprising negative emissions technologies and natural processes should aid the existing portfolio of technologies, processes, and policies, such as renewables, non-fossil fuels, clean nuclear,

energy storage, and phase-out of fossil fuels, etc., to seek peak and zero emissions, and ultimately climate restoration. The sooner we hit peak followed by zero yearly emissions, the less CO_2 we must remove. All efforts should be made to hit peak, followed by zero yearly emissions, as soon as possible to start the removal of potentially exceeding 1.5 to 2.4 trillion tonnes of carbon dioxide as shown in Equations 5, 4.

7. Error and Uncertainties

All measured data has an uncertainty of up to one standard deviation. Uncertainty for the cumulative anthropogenic fossil fuel emissions is ± 5% from the Global Carbon Budget 2017 (Le Quéré et al., 2018) and CDIAC (Boden et al., 2017). '*Generally, […] mature economies […] have uncertainties of a few percent[s] while developing countries such as China have uncertainties around ± 10%.*' (Le Quéré et al., 2018). Overall, a medium confidence was given to the fossil fuel emissions dataset, as it was generated indirectly from energy data (Durant et al., 2011) and includes per-country data variation. Land-use change emissions uncertainty is estimated at ± 0.7 GtC per year and was assigned a low confidence due to *'the inconsistencies among estimates and the difficulties to quantify some of the processes in DGVMs'* (Le Quéré et al., 2018). For the natural sinks: the land sink uncertainty for the Dynamic Global Vegetation Models (DGVMs) averages to ±0.8 GtC per year from 1959 to 2016 and has a medium confidence level. The ocean surface water sink uncertainty yearly change is ±0.5 GtC and given a medium confidence. The atmospheric annual growth uncertainty has a mean of 0.61 GtC per year for 1959-1979 and 0.19 GtC per year for 1980-2016 and was given a high confidence given the direct measurements comprising the datasets. The historical atmospheric CO_2 concentration from 1750-1959 has an uncertainty of ±3 ppm converted to ±1σ, from the Law Dome ice core data (Joos et al., 2008).

The 1980 - 2017 CO_2 concentration from Mauna Loa provided by NOAA/ESRL is listed with an uncertainty of 0.10 ppm. Antarctic Law Dome ice core data spline has an uncertainty of 1.2 ppm for 1-2004 CE (Etheridge et al., 1996; 2010), and individual ice core samples at 1.1 ppm for 1-1996 CE (MacFarling Meure et al., 2006). The Antarctic ice core data points for EPICA Dome Concordia (Dome C) (Monnin et al., 2001; Luthi et al., 2008), Vostock (Petit et al., 1999; Pépin et al., 2001; Siegenthaler et al., 2005; Luthi et al., 2008), Taylor Dome (Indermühle et al., 2001), WAIS Divide (Bauska et al., 2015), Maud Land and the South Pole (Siegenthaler et al., 2017), have uncertainty ranging from 0.1 ppm up to 2.62 ppm, a mean uncertainty of 0.8 ppm. For convenience, the combined datasets and individual uncertainties are listed in the Antarctic Historicals and graph tabs in the spreadsheet Total Emitted Carbon Graphs and Comparisons.

The CO_2 concentration baseline of 280.9 ppm from 600 BCE to 1750 CE has an average uncertainty of 0.9 ppm for the non-splined ice core data points from Dome C (Monnin et al., 2001; Luthi et al., 2008), Law Dome (Etheridge et al., 1996; MacFarling Meure et al., 2006), WAIS Divide (Bauska et al., 2015), Maud Dome and the South Pole (Siegenthaler et al., 2017). The Mauna Loa records show slightly elevated concentrations over the modern Law Dome readings and, as a precaution, lower the confidence level slightly to medium-high.

The hypothetical declines introduced in this paper are extrapolated from composites of the measured data, are speculative, and have a high uncertainty.

8. Competing Interests

Shannon Fiume runs Open NanoCarbon (received $100 USD in total donations), a presently unfunded non-profit effort doing open science research and development to solidify carbon from atmospheric CO_2, with the charter to help enable complete climate restoration by removing the total accumulated anthropogenic emitted carbon dioxide.

9. Acknowledgments

The Global Carbon Budget has been instrumental in writing this paper and its inspiration. Shannon thanks the GCB authors, NOAA and CSIRO for the ice core data and Scripps and NSF, Earth Network, for Mauna Loa data. Shannon additionally

thanks Peter Fiekowsky, Robert Cormia, Carole Douglis, the Open NanoCarbon Anonymous donor, Matt Eshed, Susan Lee, Eric Harley, Andy Lee, and everyone who's commented on the paper, and those working to restore the climate.

10. References

1. Ballantyne, A.P., Alden, C.B., Miller, J.B., Tans, P.P., and White, J.W.C., (2012), Increase in observed net carbon dioxide uptake by land and oceans during the past 50 years., *Nature*, **488**, pp. 70–72 (02 August 2012), DOI: 10.1038/nature11299

2. Bauska, T.K.; Joos, F.; Mix, A.C.; Roth, R.; Ahn, J.; Brook, E.J. (2015), Links between atmospheric carbon dioxide, the land carbon reservoir and climate over the past millennium, *Nature Geoscience*, **8**, pp. 383–387, DOI: 10.1038/ngeo2422,

a. (https://www1.ncdc.noaa.gov/pub/data/paleo/icecore/antarctica/wais2015co2.txt),

b. https://www.ncdc.noaa.gov/paleo-search/study/18316

3. Boden, T.A., Andres, R.J., Marland, G., (2017), Global, Regional, and National Fossil-Fuel CO_2 Emissions, (http://cdiac.ornl.gov/trends/emis/overview_2014.html), Carbon Dioxide Information Analysis Center, Oak Ridge National Laboratory, Department of Energy, Tennessee

4. Dlugokencky, E., Tans, P., and Keeling R., (2018), Mauna Loa Globally Averaged Yearly CO_2 ppm, Earth Science Research Laboratory, National Oceanic and Atmospheric Administration, Scripps Institution of Oceanography

a. http://www.esrl.noaa.gov/gmd/ccgg/trends/, ftp://aftp.cmdl.noaa.gov/products/trends/co2/co2_annmean_gl.txt,

5. Durant, A. J., Le Quéré, C., Hope, C., and Friend, A. D., (2011), Economic value of improved quantification in global sources and sinks of carbon dioxide, *Phil. Trans. A,* **369**, pp. 1967-1979, DOI: 10.1098/rsta.2011.0002

6. Etheridge, D.M., Steele, L.P., Langenfelds, R.L., Francey, R.J., Barnola, J.‐M. and Morgan, V. I. (1996), Natural and anthropogenic changes in atmospheric CO_2 over the last 1000 years from air in Antarctic ice and firn, *J. Geophys. Res.*, **101(D2)**, pp. 4115–4128, DOI: 10.1029/95JD03410

7. Etheridge, D.M. et al. (2010), Law Dome Ice Core 2000-Year CO_2, CH_4, and N_2O Data, IGBP PAGES/World Data Center for Paleoclimatology, Data Contribution Series # 2010-070, NOAA/NCDC Paleoclimatology Program, Boulder CO, USA

a. http://cdiac.ess-dive.lbl.gov/trends/co2/ice_core_co2.html ftp.ncdc.noaa.gov/pub/data/paleo/icecore/antarctica/law/law2006.txt

8. Flückiger, J., Monnin, E., Stauffer, B., Schwander, J., Stocker, T. F., Chappellaz, J., Raynaud, D., and Barnola, J.‐M., (2002), High‐resolution Holocene N_2O ice core record and its relationship with CH_4 and CO_2, *Global Biogeochem. Cycles*, **16(1)**, pp. 10-1-10-8, DOI: 10.1029/2001GB001417

9. Hansen, J., Sato, M., Kharecha, P., Beerling, D., Berner, R., Masson-Delmotte, V., Pagani, M., Raymo, M., Royer, D. L., and Zachos, J. C., (2008), Target Atmospheric CO_2: Where Should Humanity Aim?, *The Open Atmospheric Science Journal*, **2**, pp. 217-231, DOI: 10.2174/1874282300802010217

10. Indermühle, A., Monnin, E., Stauffer, B., Stocker, T.F., Wahlen, M. (2001), Atmospheric CO_2 concentration from 60 to 20 kyr BP from the Taylor Dome Ice Core, Antarctica. *Geophysical Research Letters*, **27(5)**, pp. 735-738, DOI: 10.1029/1999GL010960

11. Joos, F. and Spahni, R., (2008), Rates of change in natural and anthropogenic radiative forcing over the past 20,000 years, *Proceedings of the National Academy of Science*, **105(5)**, pp. 1425-1430, DOI: 10.1073/pnas.0707386105

12. Le Quéré, C., Andrew, R. M., Friedlingstein, P., Sitch, S., Pongratz, J., Manning, A. C., Korsbakken, J. I., Peters, G. P., Canadell, J. G., Jackson, R. B., Boden, T. A., Tans, P. P., Andrews, O. D., Arora, V. K., Bakker, D. C. E., Barbero, L., Becker, M., Betts, R. A., Bopp, L., Chevallier, F., Chini, L. P., Ciais, P., Cosca, C. E., Cross, J., Currie, K., Gasser, T., Harris, I., Hauck, J., Haverd, V., Houghton, R. A., Hunt, C. W., Hurtt, G., Ilyina, T., Jain, A. K., Kato, E., Kautz, M., Keeling, R. F., Klein Goldewijk, K., Körtzinger, A., Landschützer, P., Lefèvre, N., Lenton, A., Lienert, S., Lima, I., Lombardozzi, D., Metzl, N., Millero, F., Monteiro, P. M. S., Munro, D. R., Nabel, J. E. M. S., Nakaoka, S.-I., Nojiri, Y., Padin, X. A., Peregon, A., Pfeil, B., Pierrot, D., Poulter, B., Rehder, G., Reimer, J., Rödenbeck, C., Schwinger, J., Séférian, R., Skjelvan, I., Stocker, B. D., Tian, H., Tilbrook, B., Tubiello, F. N., van der Laan-Luijkx, I. T., van der Werf, G. R., van Heuven, S., Viovy, N., Vuichard, N., Walker, A. P., Watson, A. J., Wiltshire, A. J., Zaehle, S., and Zhu, D. (2018), Global Carbon Budget 2017, *Earth System Science Data*, **10**, pp. 405-448, DOI: 10.5194/essd-10-405-2018

13. Luthi, D., Le Floch, M., Bereiter, B., Blunier,T., Barnola, J.-M., Siegenthaler, U., Raynaud, D., Jouzel, J., Fischer, H., Kawamura, K., and Stocker, T.F., (2008), High-resolution carbon dioxide concentration record 650,000-800,000 years before present, *Nature*, Vol. **453**, pp. 379-382, DOI: 10.1038/nature06949, https://www1.ncdc.noaa.gov/pub/data/paleo/icecore/antarctica/epica_domec/edc-co2-2008.txt

14. MacFarling Meure, C. (2004), The variation of atmospheric carbon dioxide, methane and nitrous oxide during the Holocene from ice core analysis, (Google Scholar), Ph.D. thesis, Univ. of Melbourne, Melbourne, Vic., Australia

15. MacFarling Meure, C., Etheridge, D., Trudinger, C., Steele, P., Langenfelds, R., van Ommen, T., Smith, A. and Elkins, J., (2006), Law Dome CO_2, CH_4 and N_2O ice core records extended to 2000 years BP, *Geophys. Res. Lett.*, **33**, pp. L14810, DOI: 10.1029/2006GL026152

16. Meinshausen, M., Raper, S. C. B., and Wigley, T. M. L., (2011), Emulating coupled atmosphere-ocean and carbon cycle models with a simpler model, MAGICC6 – Part 1: Model description and calibration, *Atmos. Chem. Phys.*, **11**, 1417-1456, DOI: 10.5194/acp-11-1417-2011

17. Meinshausen, M., Wigley, T. M. L., and Raper, S. C. B., (2011), Emulating atmosphere-ocean and carbon cycle models with a simpler model, MAGICC6 – Part 2: Applications, *Atmos. Chem. Phys.*,**11**, 1457–1471, DOI: 10.5194/acp-11-1457-2011

18. Monnin, E., Indermühle, A., Dällenbach, A., Flückiger, J., Stauffer, B., Stocker, T. F., Raynaud, D. and Barnola,J.‐M., (2001), Atmospheric CO_2 concentrations over the Last Glacial Termination, *Science*, **291**, pp. 112–114, DOI: 10.1126/science.291.5501.112

19. Pépin, L., Raynaud, D., Barnola, J.-M., and Loutre, M.F., (2001), Hemispheric roles of climate forcings during glacial-interglacial transitions as deduced from the Vostok record and LLN-2D model experiments, *Journal of Geophysical Research*, **106 (D23)**, pp. 31,885-31,892, DOI: 10.1029/2001JD900117

20. Petit, J.R., Jouzel, J., Raynaud, D., Barkov, N.I., Barnola, J.-M., Basile, I. , Benders, M., Chappellaz, J., Davis, M., Delayque, G., Delmotte, M., Kotlyakov, V.M., Legrand, M., Lipenkov, V.Y., Lorius, C., Pépin, L., Ritz, C., Saltzman, E., and Stievenard, M., (1999), Climate and atmospheric history of the past 420,000 years from the Vostok ice core, Antarctica, *Nature*, **399**, pp. 429-436, DOI: 10.1038/20859

21. Raymo, M.E, Grant, B., Horowitz, M., and Rau, G. H., (1992), Mid-Pliocene warmth: stronger greenhouse and stronger conveyor, *Marine Micropaleontology*, **27**, pp. 313-326, DOI: 10.1016/0377-8398(95)00048-8

22. Riahi, K., van Vuuren, D.P., Kriegler, E., Edmonds, J., O'Neill, B.C., Fujimori, S., Bauer, N. Calvin, K., Dellink, R., Fricko, O., Lutz, W., Popp, A., Cuaresma, J.C., KC, S., Leimbach, M., Jiang, L., Kram, T., Rao, S., Emmerling, J., Ebi, K., Hasegawa, T., Havlik, P., Humpendöder, F., Da Silva, L.A., Smith, S., Stehfest, E., Bosetti, V., Eom, J., Gernaat, D., Masui, T., Rogelj, J., Strefler, J., Drouet, L., Krey, V., Luderer, G., Harmsen, M., Takahashi, K., Baumstark, L., Doelman, J.C., Kainuma, M., Klimont, Z., Marangoni, G., Lotze-Campen, H., Obersteiner, M., Tabeau, A., Tavoni, M., (2016), The Shared Socioeconomic Pathways and their energy, land use, and greenhouse gas emissions implications: An overview, *Global Environmental Change*, **42**, pp. 153-168 , DOI: 10.1016/j.gloenvcha.2016.05.009

23. Sabine, C. L, Feely, R. A, Gruber, N. Key, R. M., Lee, K., Bullister, J. L, Wanninkhof, R., Wong, C. S., Wallace, D. W. R, Tilbrook, B., Millero, F. J, Peng, T., Kozyr, A., Ono, T. and Rois, A. F., (2004), The Oceanic Sink for Anthropogenic CO_2, *Science*, **305(5682)**, pp. 367-371, DOI: 10.1126/science.1097403

24. Siegenthaler, U., Stocker, T.F., Monnin, E., Lüthi, D., Schwander, J., Stauffer, B., Raynaud, D., Barnola, J-M., Fischer, H., Masson-Delmotte, V., and Jouzel, J., (2005), Stable Carbon Cycle-Climate Relationship During the Late Pleistocene, *Science*, **310**, pp. 1313-1317, DOI: 10.1126/science.1120130

25. Siegenthaler, U., Monnin, E., Kawamura, K., Spahni, R., Schwander, J., Stauffer, B., Stocker, T.F., Barnola, J.M., and, Fischer, H., (2017), Supporting evidence from the EPICA Dronning Maud Land ice core for atmospheric CO_2 changes during the past millennium, *Tellus B: Chemical and Physical Meteorology*, **57:1**, pp. 51-57, DOI: 10.3402/tellusb.v57i1.16774,

26. SSP Public Database version 1.1 (2018), https://tntcat.iiasa.ac.at/SspDb

27. Takahashi, T., Sutherland, S. C., Sweeney, C. Poisson, A., Metzl, N., Tilbrook, B., Bates, N., Wanninkhof, R., Feely, R. A., Sabine, C., Olafsson, J., and Nojiri, Y., (2002), Global sea-air CO_2 flux based on climatological surface ocean pCO_2, and seasonal biological and temperature effects, *Deep Sea Research Part II: Topical Studies in Oceanography,* **49 (9–10)**, pp. 1601-1622, DOI: 10.1016/S0967-0645(02)00003-6

28. van Vuuren, D.P., Stehfest, E., Gernaat, D.E.H.J., Doelman, J.C., van den Berg, M., Harmsen, M., de Boer, H.S., Bouwman, L.F., Daioglou, V., Edelenbosch, O.Y., Girod, B., Kram, T., Lassaletta, L., Lucas, P.L., Meijl, H., Müller, C., van Ruijven, B.J., van der Sluis, S., Tabeau, A., (2016), Energy, land-use and greenhouse gas emissions trajectories under a green growth paradigm, *Global Environmental Change*, (**42**), pp. 237-250, DOI: 10.1016/j.gloenvcha.2016.05.008